

# Interface State Density in Atomic Layer Deposited SiO<sub>2</sub>/β-Ga<sub>2</sub>O<sub>3</sub> (2̄01) MOSCAPs

Ke Zeng, Ye Jia, and Uttam Singiseti, *Member, IEEE*

**Abstract**—The interface state density ( $D_{it}$ ) at the interface between β-Ga<sub>2</sub>O<sub>3</sub> (2̄01) and atomic layer deposited (ALD) SiO<sub>2</sub> dielectric is extracted using Terman method and conductance method. The effect of the different surface treatments on the extracted  $D_{it}$  was also studied. It is observed that the extracted  $D_{it}$  of  $6 \times 10^{11} \text{ cm}^{-2}\text{eV}^{-1}$  for the sample with no surface treatment is lower than hydrofluoric and hydrochloric acid treated samples. Low  $D_{it}$  sample shows narrow peak in the conductance method, suggesting a smooth interface. The extracted low  $D_{it}$  makes ALD SiO<sub>2</sub> an attractive candidate for future Ga<sub>2</sub>O<sub>3</sub> power devices.

**Index Terms**—Gallium oxide, ALD silicon dioxide, interface state, conductance method, Terman method.

## I. INTRODUCTION

WIDE bandgap semiconductor β-Ga<sub>2</sub>O<sub>3</sub> (Ga<sub>2</sub>O<sub>3</sub>) has recently attracted a lot of attention due to its potential for next generation power electronics. Ga<sub>2</sub>O<sub>3</sub> has been reported to have high Baliga's Figure of Merit (BFoM), a figure of merit for power devices, next to diamond among all the commonly studied wide bandgap semiconductor materials [1]. Besides excellent material properties, a mature growth technology for large area substrates is another practical advantage for cost effectiveness [2], [3]. MOSFETs and Schottky diodes based on β-Ga<sub>2</sub>O<sub>3</sub> with high breakdown voltages have been successfully demonstrated [4], [5]. In these devices, atomic layer deposited Al<sub>2</sub>O<sub>3</sub> has been used as the gate barrier due to its high dielectric constant and large conduction band-offset. However, it was recently reported that SiO<sub>2</sub>/Ga<sub>2</sub>O<sub>3</sub> interface has a much bigger conduction band offset than that of Al<sub>2</sub>O<sub>3</sub>/Ga<sub>2</sub>O<sub>3</sub> [6]. Large conduction bandoffset can reduce gate leakage and therefore, can potentially improve the device performance. Besides bandoffset, the electrical properties of the interface will also impact device performance [7]. In particular, the interface state density ( $D_{it}$ ) not only affects the gate modulation of the channel creating threshold voltage ( $V_{th}$ ) instability, but also plays a role in the variation of channel mobility. In order to reach full potential of SiO<sub>2</sub>/Ga<sub>2</sub>O<sub>3</sub> based power devices, the interface state density needs to be characterized. In this letter, interface state densities of SiO<sub>2</sub>/Ga<sub>2</sub>O<sub>3</sub>

Manuscript received April 28, 2016; accepted May 17, 2016. Date of publication May 18, 2016; date of current version June 24, 2016. This work was supported by the Office of Naval Research under Grant N000141310214. The review of this letter was arranged by Editor D. G. Senesky.

The authors are with the Electrical Engineering Department, University at Buffalo, The State University of New York, Buffalo, NY 14260 USA (e-mail: uttamsin@buffalo.edu).

Color versions of one or more of the figures in this letter are available online at <http://ieeexplore.ieee.org>.

Digital Object Identifier 10.1109/LED.2016.2570521

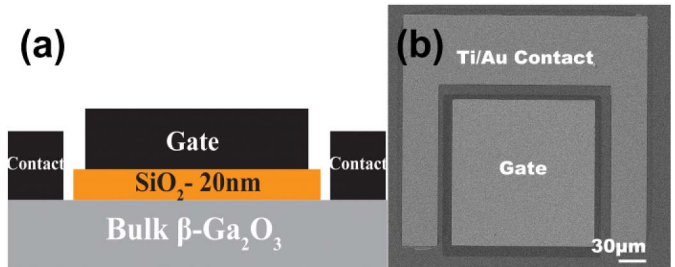


Fig. 1. (a) Cross section schematic of MOSCAP structure. (b) SEM image of fabricated  $100 \mu\text{m} \times 100 \mu\text{m}$  MOSCAP.

metal oxide semiconductor (MOS) structure with different surface treatment are investigated by two methods: Terman method and conductance method. The implication of the data and the limitations of methods are also discussed.

## II. EXPERIMENTS

MOS capacitance (MOSCAP) structures, shown in Fig. 1(a), with different sizes were used here for interface state density characterization. The interface state density at semiconductor/dielectric interfaces have been reported to decrease with various surface treatments [8]. To study the effect of wet chemical surface treatment, samples with hydrofluoric (HF) and hydrochloric (HCl) acid surface treatment have been analyzed together with samples with no treatment. The Ga<sub>2</sub>O<sub>3</sub> substrates studied here were grown by Tamura Corporation with a Sn doping density of  $9 \times 10^{18}/\text{cm}^3$ . Three bare β-Ga<sub>2</sub>O<sub>3</sub> samples were cleaved from this substrate and the samples were cleaned in standard solvents and rinsed in deionized (DI) water. One was then dipped in HF for 1 minutes, another dipped in HCl for 1 minutes and both were subsequently rinsed for 1 minute in deionized (DI) water. The treatment of HF and HCl did not create any visible chemical reaction and no measurable etching was observed in atomic force microscopy (AFM) analysis. The measured root mean square surface roughness for all the samples was  $\sim 0.2\text{-}0.3 \text{ nm}$ . A 20 nm layer of SiO<sub>2</sub> was then deposited by atomic layer deposition (ALD) for all three samples at the same time. The thickness of the deposited SiO<sub>2</sub> film was verified on a Si monitor wafer by spectroscopic ellipsometer. For MOSCAP fabrication, the Ti/Au gate electrodes were first defined by standard photolithography and lift-off procedure. Then, silicon dioxide layer was etched away by CF<sub>4</sub>/O<sub>2</sub> based reactive ion etching (RIE) at contact regions. Before deposition of Ti/Au ohmic contacts, a BCl<sub>3</sub>/Ar etch was performed. Then Ti/Au contact metals were deposited, followed by annealing at 470 °C for 1 minutes to make

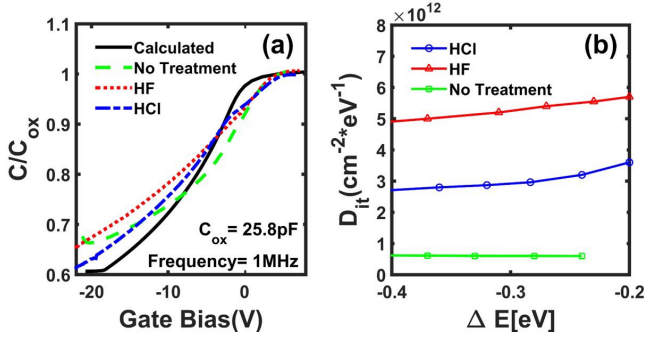


Fig. 2. (a) Comparison of calculated ideal C-V and measured C-V curves of samples with different surface treatment. (b) Interface trap density  $D_{it}$  versus energy level  $\Delta E$  derived from C-V measurement using Terman method for three samples. Size of the MOSCAP is  $100 \mu\text{m} \times 150 \mu\text{m}$ .

the contacts ohmic [4]. Scanning electron microscope (SEM) image of one fabricated device is shown in Fig. 1(b).

### III. RESULTS AND DISCUSSION

The interface state density was first extracted using Terman method [9]. In this method, a measured high frequency (hf) C-V curve is compared with an ideal calculated C-V curve to generate interface trap density distribution over bandgap. The ideal C-V curve was calculated numerically using MATLAB [11] from the exact solution of the electrostatics model of the MOSCAP with a doping density of  $9 \times 10^{18} \text{ cm}^{-3}$ . Deep depletion was included in the calculation [12]. The band alignment parameters reported in [6] was used in the calculations. The hf C-V was measured at 1 MHz frequency assuming the interface traps do not respond to the hf ac excitation, but will follow the slowly varying dc bias. Fig. 2(a) shows the calculated C-V curve and measured 1 MHz C-V curves from  $100 \mu\text{m} \times 150 \mu\text{m}$  devices. The flat band voltage ( $V_{FB}$ ) evaluated from the C-V curve is  $\sim 5.1 \text{ V}$  which gives an oxide trapped sheet charge density of  $5.5 \times 10^{12} \text{ cm}^{-2}$ . The horizontal stretch out of the measured curves in the figure is an indication of interface state density response to the slowly varying gate bias. It can be seen that the stretch out of the sample with no treatment is lower than HF and HCl treated samples, indicating a lower  $D_{it}$ . The interface trap density can be determined from the stretch out of the measured curves by [9]:

$$D_{it} = \frac{C_{ox}}{q^2} \left( \frac{dV_g}{d\phi_s} - 1 \right) - \frac{C_s}{q} = \frac{C_{ox}}{q^2} \frac{d\Delta V_g}{d\phi_s}, \quad (1)$$

where  $\Delta V_g = V_g$  (measured) -  $V_g$  (ideal), and  $\phi_s$  is surface potential and  $C_s$  is semiconductor capacitance. In the simulated ideal C-V curve, each gate bias  $V_g$  correspond to a surface potential  $\phi_s$ . Therefore, calculated  $D_{it}$  at each  $\phi_s$  point can generate a plot of  $D_{it}$  vs.  $\Delta E$ . However, the energy range where the Terman method gives accurate  $D_{it}$  is significantly limited by the hf ac frequency and dc sweep rate [14]. With ac frequency of 1 MHz and a dc sweep rate of  $\sim 3 \text{ V/s}$ , only traps between 0.2 and 0.4 eV below conduction band can be accurately measured and they are shown in Fig. 2(b).

Fig. 2(b) also shows that HCl and HF treated MOSCAPs have comparable  $D_{it}$ , while sample with no treatment shows

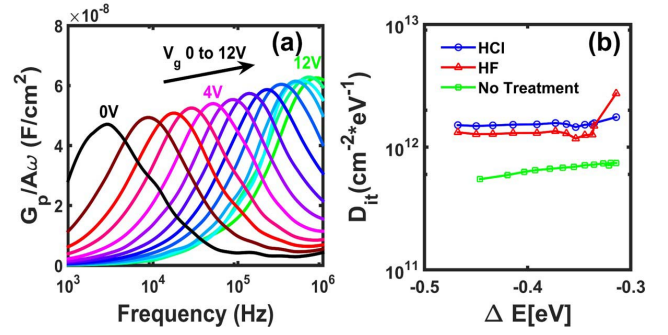


Fig. 3. (a) Normalized equivalent conductance spectrum at various gate bias derived from measured conductance data for the sample with no treatment. (b) Interface trap density  $D_{it}$  versus energy level  $\Delta E$  derived from the peak value of normalized conductance spectrum. Conductance was measured at 300K. Size of the MOSCAP is  $100 \mu\text{m} \times 150 \mu\text{m}$ .

lower  $D_{it}$ . The  $D_{it}$  extracted from Terman method for sample with no treatment, HF treated and HCl treated samples are  $6.5 \times 10^{11} \text{ cm}^{-2} \text{ eV}^{-1}$ ,  $4.9 \times 10^{12} \text{ cm}^{-2} \text{ eV}^{-1}$  and  $2.7 \times 10^{12} \text{ cm}^{-2} \text{ eV}^{-1}$  respectively, at 0.4 eV below conduction band. Terman method has been most critiqued for the uncertainty of generated ideal C-V curve and also due to the C-V curve stretch out by the border traps [9]. Also, in the calculation of ideal C-V curve, the slope changes significantly with doping density  $N_D$  which adds some uncertainty to the result. However, as described in section II, all the three samples reported here were fabricated on the same substrate with a constant  $N_D$ , Terman method gives good information about the relative difference of  $D_{it}$  on the three samples.

The  $D_{it}$  was also extracted using conductance method. Compared to Terman method, conductance method is much slower and requires higher precision of measurement but has been shown to be very accurate for determining  $D_{it}$  in semiconductor interfaces [10], [13]. However, the  $D_{it}$  is characterized only over a narrow range in the bandgap due to the limitations of measurement temperature and frequency. At various gate biases, the ac conductance ( $G_m$ ) and the capacitance ( $C_m$ ) of the MOSCAPs were measured using Agilent 42941A impedance probe kit and Agilent 4294A from 1 kHz to 1 MHz. From the measured ac conductance, the normalized equivalent parallel conductance is calculated by [10], [13]:

$$\frac{\langle G_p \rangle}{\omega} = \frac{\omega C_{ox}^2 G_m}{G_m^2 + \omega^2 (C_{ox} - C_m)^2}, \quad (2)$$

where  $C_{ox}$  is the oxide capacitance measured in accumulation,  $G_m$  and  $C_m$  were measured conductance and capacitance respectively, and  $\omega$  is the angular frequency of measurement. The extracted equivalent conductance ( $G_p$ ) versus measurement frequency for the sample with no treatment is shown in Fig. 3(a). The sharp and narrow peaks correspond to interface states' response and the modulation of the peak position with gate bias is also as expected [14]. In addition, the peak is very narrow ( $G_{p,peak}/5$  spans only one order in bandwidth) compared to SiC/dielectric interfaces [14], which suggests a small time constant dispersion [13]. This is one of the attributes of a good interface. From the conductance peak,

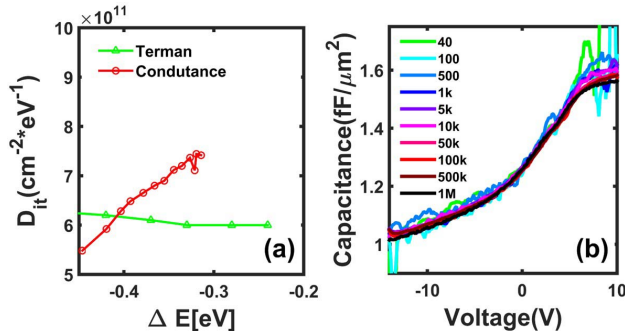


Fig. 4. (a) Combined  $D_{it}$  versus  $\Delta E$  plot for sample with no treatment. (b) Frequency dependent C-V curve for sample with no treatment 300K. It shows very small frequency dispersion. Size of the MOSCAP is  $150 \mu\text{m} \times 225 \mu\text{m}$ . DC sweep rate is 0.05 V/s.

the interface trap density can be calculated using [10]:

$$D_{it} \approx \frac{2.5}{Aq} \left( \frac{G_p}{\omega} \right)_{peak}, \quad (3)$$

where  $A$  is area of device. The location of the  $D_{it}$  in the bandgap ( $\Delta E$ ) can be calculated by Shockley–Read–Hall statistics of capture and emission rates [10],

$$\tau = \frac{\exp\left(\frac{\Delta E}{kT}\right)}{\sigma v_t N}, \quad (4)$$

where  $\tau = 2\pi/\omega$ ,  $\sigma$  is the capture cross section of the trap and the value  $1 \times 10^{-15} \text{ cm}^2$  is used [16],  $v_t$  is average thermal velocity of majority carriers,  $N$  is the effective density of states of the majority carrier band,  $k$  is the Boltzmann constant and  $T$  is the temperature. Fig. 3(b) shows the calculated  $D_{it}$  vs.  $\Delta E$  obtained from the conductance method for all the samples. It is again seen that the extracted  $D_{it}$  is lower for the sample with no treatment as compared to HF and HCl treated samples, which is consistent with Terman method result in Fig. 2(b).

Note in Fig. 3(b), the characterized trap energy range is very close to conduction band because the samples were measured at room temperature. To put the two methods into perspective, Fig. 4(a) shows a combined plot of results from conductance method and Terman method for sample with no treatment. It can be seen that the results are very similar at conduction band edge.

Fig. 4(b) shows the frequency dispersion of the C-V curves for sample with no treatment, a very small dispersion of about 1% is observed over large range of frequencies (40 Hz to 1 MHz) in the depletion region ( $V_g < 5 \text{ V}$ ), which is also an indication of low  $D_{it}$  interface. Using the Hi-Lo method proposed by Castagné and Vapaille [17], the peak  $D_{it}$  is extracted from  $\Delta C$  of 1 MHz and 40 Hz CV curve at  $V_g \approx 5 \text{ V}$  to be  $2.6 \times 10^{10} \text{ cm}^{-2} \text{ eV}^{-1}$  at  $\sim 0.2 \text{ eV}$  below conduction band using:

$$D_{it} = \left( \frac{C_{ox} C_{LF}}{C_{ox} - C_{LF}} - \frac{C_{ox} C_{HF}}{C_{ox} - C_{HF}} \right) / qA, \quad (5)$$

where  $C_{ox}$  is the capacitance at accumulation,  $C_{LF}$  and  $C_{HF}$  are the measured low and high frequency CV curves. This value is lower than the value calculated from Terman and conductance method because 40 Hz is not low enough and some interface states still cannot respond to the ac signal.

The low frequency C-V in accumulation ( $V_g > 5 \text{ V}$ ) shows noise caused by the gate leakage in the 20 nm thick oxide layer.

It is noted that the  $D_{it}$  is determined close to the conduction band, the methods used here do not throw any insight on  $D_{it}$  in deep levels. Using temperature dependent C-V can further increase the range of  $D_{it}$ , but  $D_{it}$  below midgap can still not be probed due to the absence of p-type doping in  $\text{Ga}_2\text{O}_3$ . However, in a MOSFET operation,  $D_{it}$  within the range of the Fermi-level movement will influence device operation.

#### IV. CONCLUSION

In summary, we evaluated the  $\text{Ga}_2\text{O}_3$ - $\text{SiO}_2$  interface state density by MOSCAP C-V and G-V measurements. Terman method and conductance method were used to extract the  $D_{it}$ . From both methods, the interface trap density close to the conduction band is low ( $\sim 6 \times 10^{11} \text{ cm}^{-2} \text{ eV}^{-1}$ ) for the sample with no treatment. However, the  $D_{it}$  is increased for HF and HCl treated samples to  $2 \times 10^{12} \text{ cm}^{-2} \text{ eV}^{-1}$ . The low  $D_{it}$  in the untreated samples will have minimal effect on the device performance. Terman method, conductance method and low frequency dispersion indicate a good interface between  $\text{Ga}_2\text{O}_3$  and  $\text{SiO}_2$ . Although the treatment of HCl and HF did not improve the  $D_{it}$ , it provided a useful reference for future experiments. More sophisticated interface treatment, like RCA clean [16], may be required to further reduce  $D_{it}$ .

#### REFERENCES

- [1] M. Higashiwaki, K. Sasaki, A. Kuramata, T. Masui, and S. Yamakoshi, "Gallium oxide ( $\text{Ga}_2\text{O}_3$ ) metal-semiconductor field-effect transistors on single-crystal  $\beta$ - $\text{Ga}_2\text{O}_3$  (010) substrates," *Appl. Phys. Lett.*, vol. 100, no. 1, pp. 2012–2015, Jan. 2012, doi: 10.1063/1.3674287.
- [2] E. G. Villora, K. Shimamura, Y. Yoshikawa, K. Aoki, and N. Ichinose, "Large-size  $\beta$ - $\text{Ga}_2\text{O}_3$  single crystals and wafers," *J. Cryst. Growth*, vol. 270, nos. 3–4, pp. 420–426, Oct. 2004, doi: 10.1016/j.jcrysgro.2004.06.027.
- [3] Y. Tomm, P. Reiche, D. Klimm, and T. Fukuda, "Czochralski grown  $\text{Ga}_2\text{O}_3$  crystals," *J. Cryst. Growth*, vol. 220, pp. 510–514, Dec. 2000, doi: 10.1016/S0022-0248(00)00851-4.
- [4] M. Higashiwaki, K. Sasaki, T. Kamimura, M. H. Wong, D. Krishnamurthy, A. Kuramata, T. Masui, and S. Yamakoshi, "Depletion-mode  $\text{Ga}_2\text{O}_3$  metal-oxide-semiconductor field-effect transistors on  $\beta$ - $\text{Ga}_2\text{O}_3$  (010) substrates and temperature dependence of their device characteristics," *Appl. Phys. Lett.*, vol. 103, no. 12, p. 123511, Sep. 2013, doi: 10.1063/1.4821858.
- [5] K. Sasaki, M. Higashiwaki, A. Kuramata, T. Masui, and S. Yamakoshi, " $\text{Ga}_2\text{O}_3$  Schottky barrier diodes fabricated by using single-crystal  $\beta$ - $\text{Ga}_2\text{O}_3$  (010) Substrates," *IEEE Electron Device Lett.*, vol. 34, no. 4, pp. 493–495, Apr. 2013, doi: 10.1109/LED.2013.2244057.
- [6] Y. Jia, K. Zeng, J. S. Wallace, J. A. Gardella, and U. Singiseti, "Spectroscopic and electrical calculation of band alignment between atomic layer deposited  $\text{SiO}_2$  and  $\beta$ - $\text{Ga}_2\text{O}_3$  (201)," *Appl. Phys. Lett.*, vol. 106, no. 10, p. 102107, Mar. 2015, doi: 10.1063/1.4915262.
- [7] S. Nakazawa, T. Okuda, J. Suda, T. Nakamura, and T. Kimoto, "Interface properties of 4H-SiC (1120) and (1100) MOS structures annealed in  $\text{NO}$ ," *IEEE Trans. Electron Devices*, vol. 62, no. 2, pp. 309–315, Feb. 2015, doi: 10.1109/TED.2014.2352117.
- [8] T.-H. Hung, P. S. Park, S. Krishnamoorthy, D. N. Nath, and S. Rajan, "Interface charge engineering for enhancement-mode GaN MISHEMTs," *IEEE Electron Device Lett.*, vol. 35, no. 3, pp. 312–314, Mar. 2014, doi: 10.1109/LED.2013.2296659.
- [9] D. K. Schroder, *Semiconductor Material and Device Characterization*, 3rd ed. New York, NY, USA: Wiley, 2006.
- [10] R. Engel-Herbert, Y. Hwang, and S. Stemmer, "Comparison of methods to quantify interface trap densities at dielectric/III–V semiconductor interfaces," *J. Appl. Phys.*, vol. 108, no. 12, p. 124101, Dec. 2010, doi: 10.1063/1.3520431.

- [11] R. F. Pierret, *Semiconductor Device Fundamentals*, 2nd ed. Reading, MA, USA: Addison-Wesley, 1996.
- [12] P. Friedrichs, E. P. Burte, and R. Schörner, "Interface properties of metal-oxide-semiconductor structures on *n*-type 6H and 4H-SiC," *J. Appl. Phys.*, vol. 79, no. 10, p. 7814, Feb. 1996, doi: 10.1063/1.362389.
- [13] E. H. Nicollian and A. Goetzberger, "The Si-SiO<sub>2</sub> interface—Electrical properties as determined by the metal-insulator-silicon conductance technique," *Bell Syst. Tech. J.*, vol. 46, no. 6, pp. 1055–1133, Jul. 1967, doi: 10.1002/j.1538-7305.1967.tb01727.x.
- [14] J. A. Cooper, Jr., "Advances in SiC MOS technology," *Phys. Status Solidi A*, vol. 162, pp. 305–320, Jan. 1997, doi: 10.1002/1521-396X(199707)162:1<305::AID-PSSA305>3.0.CO;2-7.
- [15] J. N. Shenoy, G. L. Chindalore, M. R. Melloch, J. A. Cooper, J. W. Palmour, and K. G. Irvine, "Characterization and optimization of the SiO<sub>2</sub>/SiC metal-oxide semiconductor interface," *J. Electron. Mater.*, vol. 24, no. 4, pp. 303–309, Oct. 1995, doi: 10.1007/BF02659691.
- [16] G. Brammertz, K. Martens, S. Sioncke, A. Delabie, M. Caymax, M. Meuris, and M. Heyns, "Characteristic trapping lifetime and capacitance-voltage measurements of GaAs metal-oxide-semiconductor structures," *Appl. Phys. Lett.*, vol. 91, no. 13, p. 133510, Sep. 2007, doi: 10.1063/1.2790787.
- [17] R. Castagné and A. Vapaille, "Description of the SiO<sub>2</sub>-Si interface properties by means of very low frequency MOS capacitance measurements," *Surf. Sci.*, vol. 28, no. 1, pp. 157–193, 1971, doi: 10.1016/0039-6028(71)90092-6.